# Failure Analysis of a New Turbine Parting Plane Stud

H. Roy*, A. Saha, D.Ghosh, S. Ray and A.K. Shukla

*Central Mechanical Engineering Research Institute, CSIR, Durgapur-713209, India*

## ABSTRACT

This investigation was primarily aimed to examine the probable causes of failure of a new turbine parting plane stud. The stud made from X22CrMoV121 grade steel failed from the threads (nut side) during assembly. Preliminary visual examination, evaluation of thread profile, evaluation of mechanical properties, detailed optical and scanning electron microscopy analysis were the necessary supplements to this investigation. Finally, it was concluded that as the stud was electrically heated through the central bore during tightening, faulty electrical practice might have caused an electric spark at isolated locations leading to cracks.

**Keywords:** Stud; Failure; Inclusion; SEM; Carburized layer; Crater

## 1. INTRODUCTION

Generation of power in a thermal power plant is done through a turbine which is composed of a rotor consisting of several rows of closely spaced blades, fixed vanes, casing and boltings. The various turbine sections are enclosed in a massive steel casing or shells which are usually made into halves bolted together. The function of the casing is two folds i.e. contenting the steam pressure and maintaining supported alignment of the internal components. A steam turbine casing has many bolted joints using different sizes of studs, which also facilitate the maintenance or repair work, and are exposed to a working temperature of up to 570°C. The basic function of the studs is to maintain the steam tied joints to the creep range without relaxing or fracturing. The elastic strains produced by the initial tightening of the studs are progressively converted to creep strains, thereby reducing the load carrying capacity. Studs are usually tightened to a pre-defined cold strength of about 1.05%. The tightening intervals of the studs are pre-calculated and in general vary between 6-8 intervals /1/. Fixing of the new studs is always accompanied with a uniform heating, so as to tighten them up to the limit of the design load. The heating of the studs in some crude cases is being done by using hot gases passing through the holes of the studs and maintaining uniform temperature throughout the section. The recent trend for tightening is to heat the stud using an inserted coil and maintain the

*Tel.: +91-343-6452085. Fax: +91-343-2546745.
E-mail address: h_roy@cmeri.res.in, himadri9504@gmail.com

temperature during the tightening process. This is basically the closure procedure for inner and outer casing of turbines. Fracture of the studs is mainly caused due to metallurgical reasons, i.e. embrittlement /2-4/, poor design or poor tightening procedures but the important phenomena are associated always with creep rupture and brittle fracture /1/.

This investigation has been carried out on a new parting plane turbine stud that failed during the assembly process. The following as-received samples were investigated: (a) failed stud containing both the fracture surfaces (b) one nut and (c) one sleeve. The samples in the as-received condition are shown in Figure 1. The material of the stud was X22CrMoV121 grade steel (Table 1) and it was electrically heated through the central bore during tightening. The measured value of thread profile conforms to DIN specification 2510 Pt.2 (Table 2) except for the root radius.

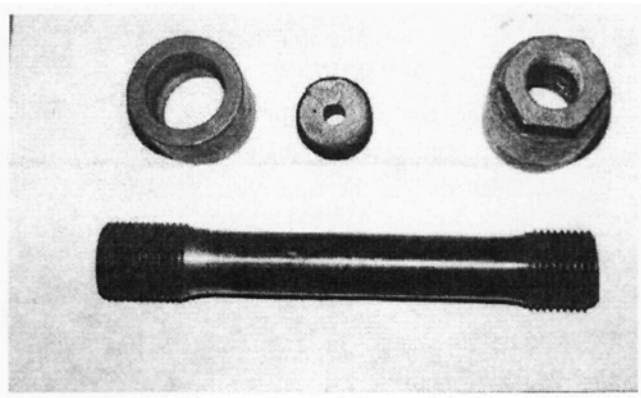

**Fig. 1:** As received failed stud samples.

**Table 1**
Chemical composition (wt%) of the failed stud.

| Elements | C | Cr | Ni | Mo | V |
|---|---|---|---|---|---|
| Composition | 0.60 (Surface)<br>0.20 (Core) | 0.27 | 1.13 | 0.20 | 95.57 |

**Table 2**
Measured and specified values of thread profile

| Thread Elements | Measured Values | Specified limit (As per DIN 2510 Pt.2) |
|---|---|---|
| Mean Pitch radius | 6.001 mm | 6.000 (nominal) |
| Root radius | No continuous root radius | 15.24 nm |
| Outside diameter | 71.511 mm | 71.046-71.646 mm |
| Effective diameter | 64.822 mm | 67.469-67.749 mm |
| Minor diameter | 63.634 mm | 63.573-64.285 mm |
| Mean included angle | $57^0 48'$ | $60^0$ |

## 2. EXPERIMENTAL PROCEDURE

### 2.1 Visual Examination

The entire failed stud including the fracture surfaces was visually examined before cleaning. It was observed that the fracture occurred through the 7-8$^{th}$ thread from the nut end. Moreover, approximately 75% of the fractured surface was smooth without any visible deformation (Figure 2). Few radial marks were also observed on the fracture surface. Deep tool marks on the centre hole surface along with weld spatter like deposit and some pits at isolated locations could also be seen (Figure 3).

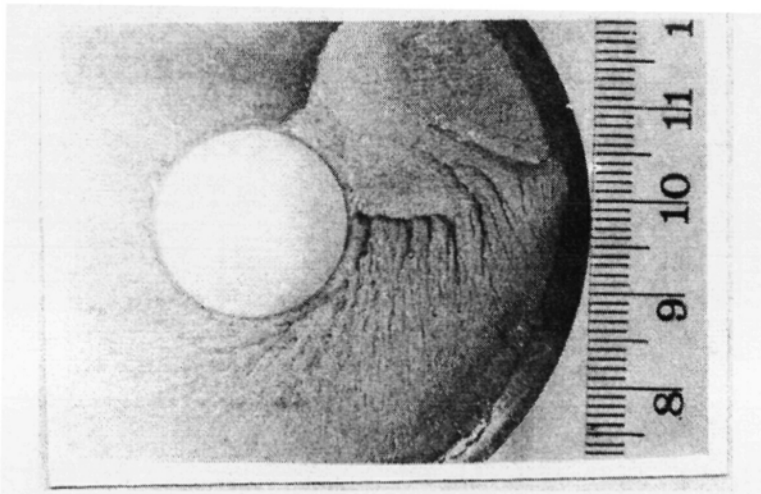


**Fig. 2:** Fracture surface of the failed stud.

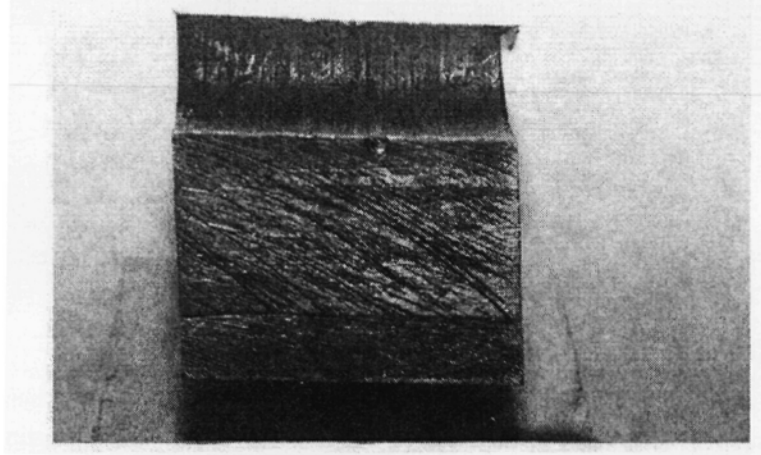

**Fig. 3:** Deep tool marks along with weld spatter deposit.

### 2.1 Sample Preparation

For conducting mechanical tests and microstructural characterization, samples were prepared from the threaded portion of the nut end, the other end, and shank of the stud, and were marked as 'A', 'B' and 'S' respectively as shown in Figure 4. The extraction of samples from the failed stud for conducting tensile and impact tests are shown in Figure 5.

The following samples were then subjected to different tests:

| | |
|---|---|
| Scanning Electron Microscopy: | A-2 (containing fracture surface) |
| Hardness measurement: | A-1 |
| Metallography and micro-hardness: | 1A4, 2A4, 3A4, 4A4, 5A4, 2B1, 3B1 4B1, 5B1, 1B4, 2B4, 1S1, 2S1 & S2 |
| Tensile test: | S1 & S4 |
| Impact test: | S2 & S3 |

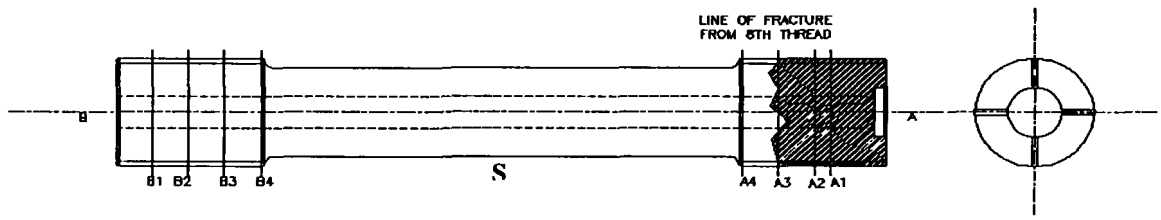


**Fig. 4:** Location of samples for SEM and Metallography

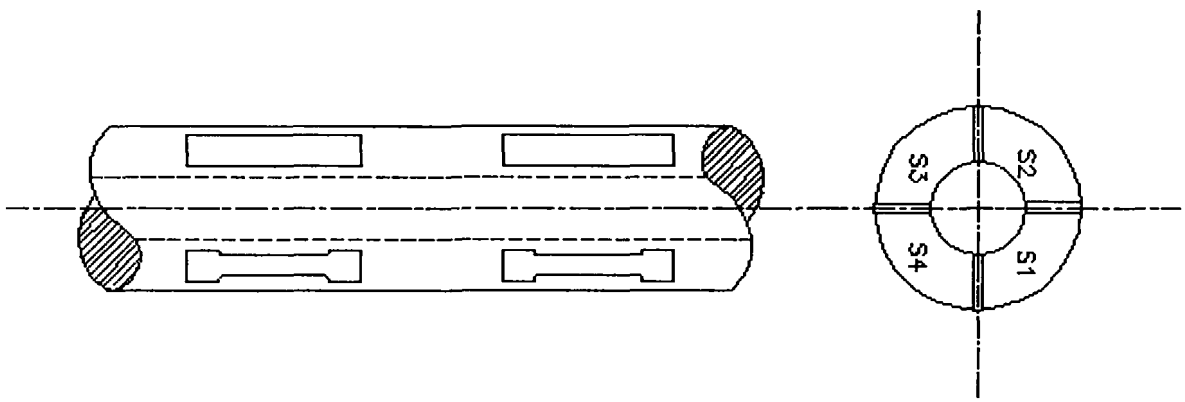


**Fig. 5:** Identification of location of samples for impact and tensile test

### 2.1 Mechanical Testing and Microstructural Characterization

Tensile testing was carried out in 6mm diameter and 30 mm gauge length specimens using an Instron testing machine [Model:5350]. Impact testing was carried out in a charpy impact testing machine [Make: AVERY, UK]. Hardness measurement was carried out on sample A1 across the cross section (outer edge to the central bore edge) using Hardness Tester 751 (Instron Wolpert, UK) in Vickers hardness scale under 20 Kgf load. Micro-hardness was also carried out using (MXT 70, Matsuzawa Seiki Ltd, Japan) of different layers at crater (sample no: 1S1) as shown in Figure 6.

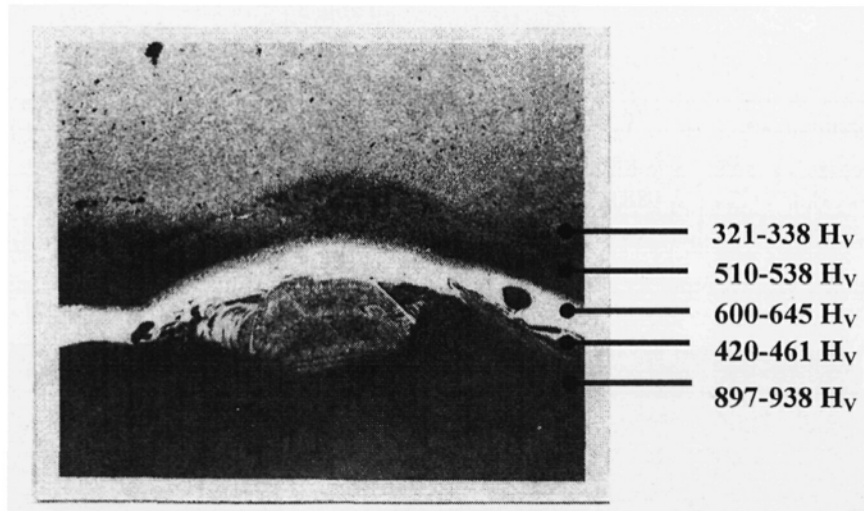


**Fig. 6:** Metallograph of the central bore surface of the stud. Microhardness measurements of the different layer has also been shown.

Small specimens were cut from the failed stud, polished up to 1000 grade emery paper followed by cloth polishing and then etched with freshly prepared nital (2 wt%). The polished and etched samples were observed under optical microscope ($MeF_3$) for evaluating the microstructural features. One of the fracture surfaces was properly cleaned using an ultrasonic cleaner and was observed under Scanning Electron Microscope (SEM). A number of representative photographs of the damaged surface and the fracture surface were taken using a Hitachi S3000 N SEM.

## 3. DISCUSSION AND CONCLUSIONS

The tensile and impact properties of the failed stud are reported in Table 3. From the observed values it was found that the tensile properties conform with the specification of the material /5/. However, the impact properties were found to be marginally lower, which can be due to the presence of inclusions in the tested samples. Unetched microstructural examination near the thread region (2A4 sample) reveals absence of thread root radius (Figure 7a) whereas the etched sample adjacent to the central bore (S2) surface showed three microscopically distinct layers on the central bore region (Figure 7b). Some pits were also observed in association with microcracks at pit root (1S1) as well as adjacent to an inclusion (Figure 7c). The etched surface revealed shallow pit with layered structure, micro voids and cracks (Figure 6). The cracks were found to be originating from the outermost cast layer on central bore surface and propagating towards the subsequent layer (Figure 7d). The outer surface of the central bore revealed a layer resembling a carburized layer, followed by tempered martensite with grain boundary carbide (Figures 8a and 8b). In the near central bore (sample A3) cracks were found to be initiating from an inclusion located within the carburized layer and propagating to the central bore surface (Figure 8c).

**Table 3**
Tensile and impact test results

| Specimen No. | Y.S ($Kg/mm^2$) | U.T.S ($Kg/mm^2$) | % El | % RA | Charpy Impact, Kg-m |
|---|---|---|---|---|---|
| 1 | 88.42 | 102.09 | 16.4 | 49.4 | 1.8 |
| 2 | 89.47 | 101.74 | 16.0 | 49.5 | 1.8 |
| 3 | 88.0 | 102.18 | 16.0 | 49.0 | 1.7 |

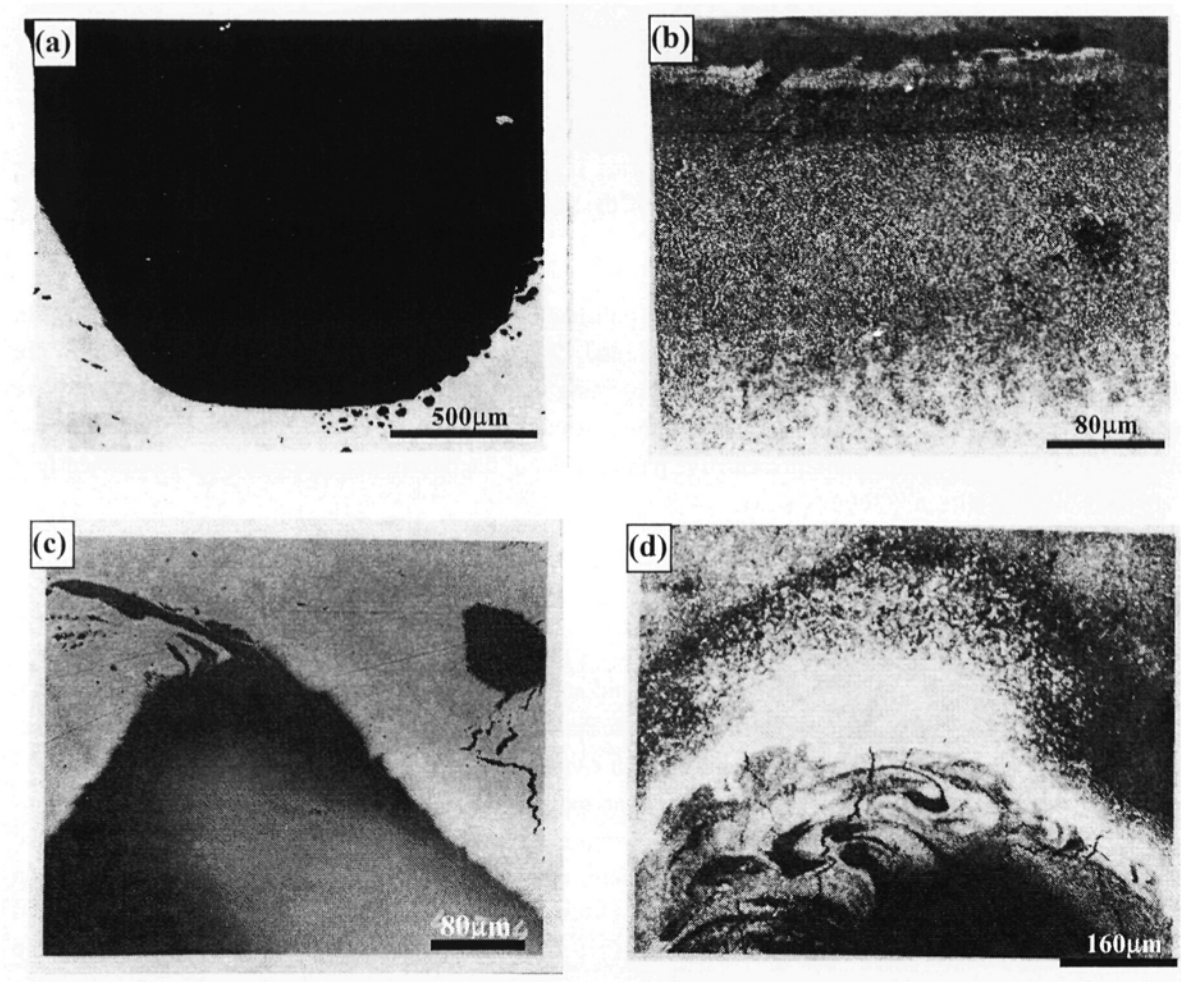


**Fig. 7:** Micrographs taken (a) near the thread root region revealing absence of thread root radius (b) near the central bore region showed three distinct etched regions (c) near the pit root showing cracks originating from the inclusion and (d) near the central bore surface showing cracks propagating along subsequent layers.

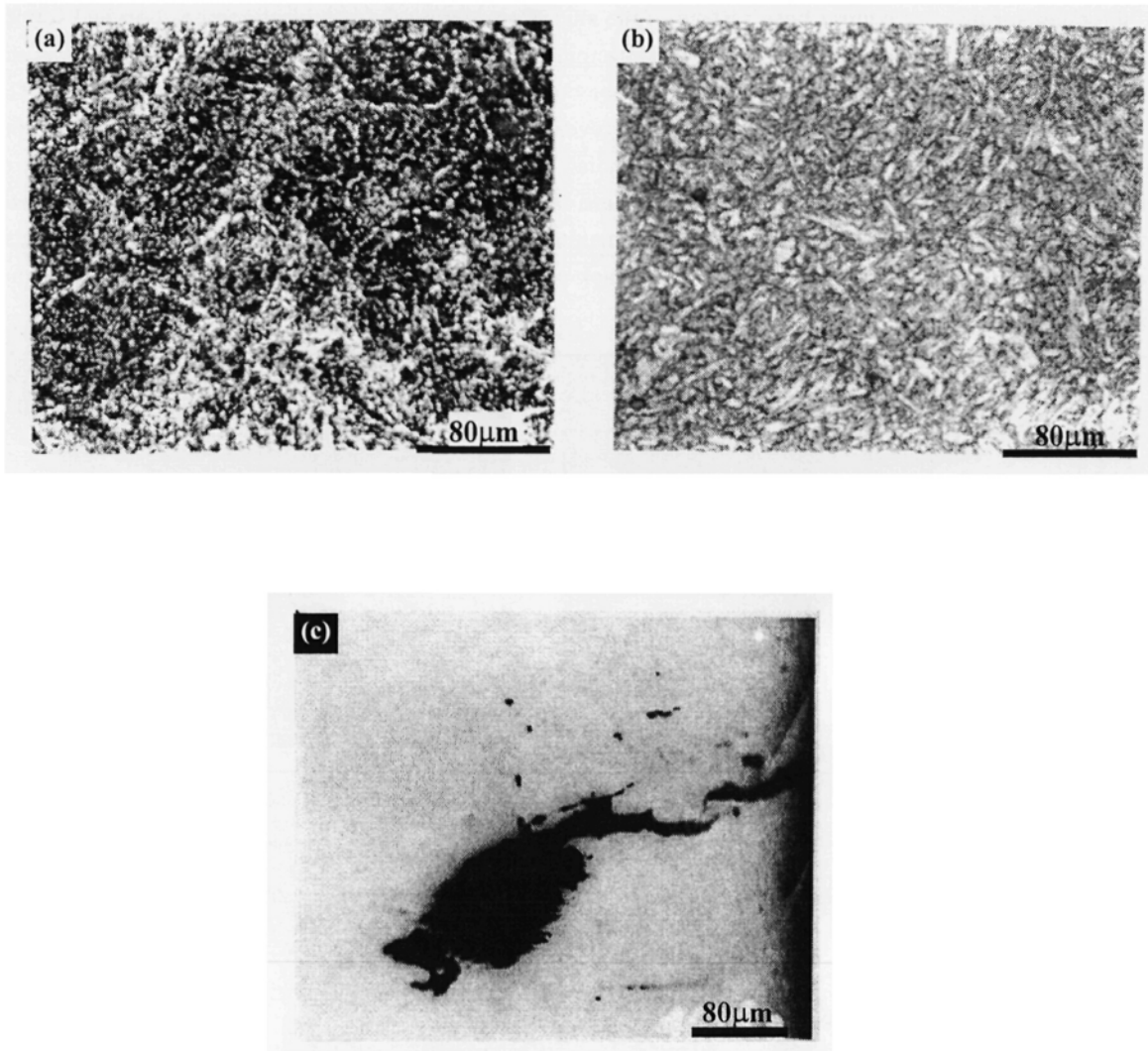


**Fig. 8:** The microstructure of the outer surface of the central bore revealed (a) grain boundary carbide followed by (b) tempered martensite. (c) Near the central bore region within the carburized layer cracks were found to initiate from inclusion.

A uniform metallographically distinguishable layer of thickness of about 0.2-0.3 mm was found both on the outer surface and on the central bore surface of the stud, where weld spatter like deposits and craters were observed (Figure 6). The microhardness examination of the observed layer (510-538 $H_V$) was found to be higher than that of the core (321-338 $H_V$). Maximum hardness (897-938 $H_V$) was observed on the outermost layer. As the microstructure of the layer resembled that of a case carburized layer, the sample obtained from the outer surface was separately processed for carbon estimation. The carbon content of the sample at hand was found to be 0.6%, in contrast to the value of 0.2% of the core material. The higher carbon content of the

sample collected from the outer surface as well as its higher measured hardness value support carburization of the outer surface and central bore surface of the stud. Considering the chemical composition and service requirements of the stud, as well as the normal engineering practice, it is thought that the stud was not intentionally carburized but resulted from improper control of furnace atmosphere during hardening. The SEM examination of one of the fracture surfaces revealed the presence of small crater on the central bore surface at the plane of fracture, the depth of the notch was about 0.8-1.0 mm, along with some amount of plastic deformation at the tip of the crater (Figure 9a). A large half elliptical macro crack of several millimetre length and almost 1 mm width at its maximum depth at the edge of the central bore was also observed (Figure 9b); just in front of the macrocrack several transverse cracks were also observed (Figure 9c).

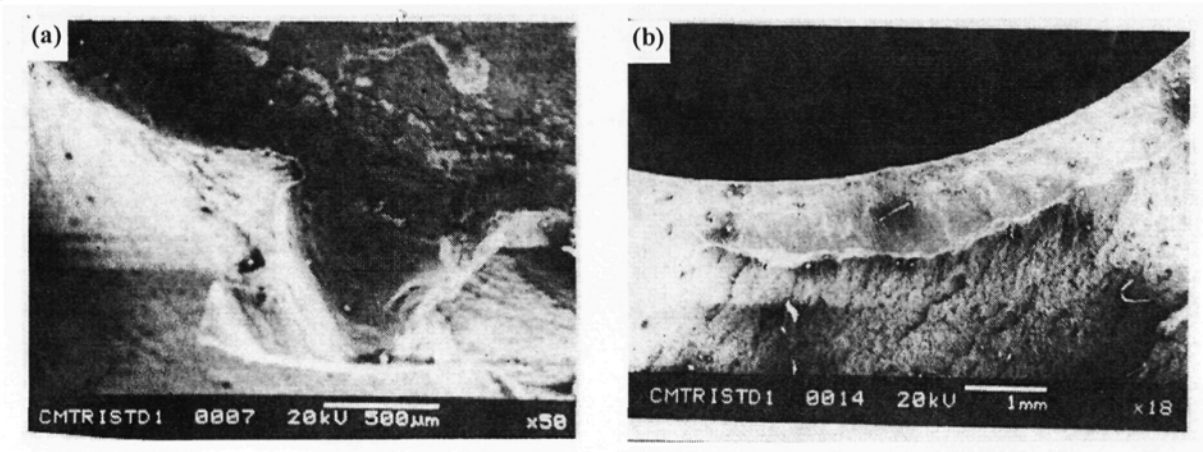


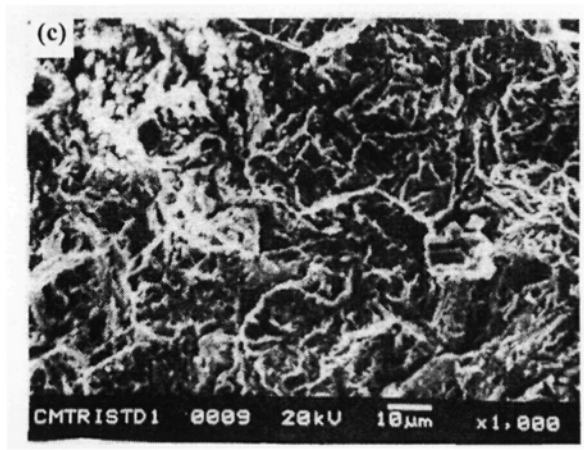


**Fig. 9:** The SEM photograph of (a) small crater on the central bore surface at the plane of fracture showing some amount of plastic deformation at the tip of the crater (b) half. Elliptical macrocrack and (c) several transverse cracks ahead of macrocrack.

To conclude, momentary intense heating, possibly due to formation of an electrical spark at the time of heating the stud through the central bore during assembly, caused adverse metallurgical conditions of the material of the stud at isolated locations on the surface of the central bore as well as formation of craters and cracks leading to failure of the stud. Adverse effect of thermal stress and metallurgical changes due to faulty heating was aggravated by the presence of a brittle carburized layer on the central bore surface as well as the presence of inclusions in the material. The cracks initiated from the brittle carburized layer and traversed towards the surface of the central bore leading to its failure.

## REFERENCES

1. Viswanathan, R, Damage mechanisms and life assessment of high temperature components, ASM International, Metals Park, Ohio, 1989.
2. Low, J.R. Jr., Stein, D.F., Turkalo, A.M., and Laforce, R.P., Alloy and impurity effects on temper brittleness of steel, *Trans. Metal. Soc. AIME* **242**, 14-24, 1968.
3. Chowdhury, S.G., Kumar, P., Das, S.K., Bhattacharya, D.K. and Parida, N., Failure analysis of high temperature studs, *Engng. Fail Anal.* **8**, 521-528, 2001.
4. Yu, J. and Mcmahon, C.J., The effects of composition and carbide precipitation on temper embrittlement of 2.25 Cr-1 Mo steel: Part II. Effects of Mn and Si, *Metall. Trans. A.* **11**, 291-300, 1980.
5. Materials Handbook, Vol.1, 10th edition, ASM International, 1991.